ACS chemical biology

Letters

pubs.acs.org/acschemicalbiology

Wild Type, Mutant Protein Unfolding and Phase Transition Detected by Single-Nanopore Recording

Céline Merstorf,[†,#] Benjamin Cressiot,[†,#] Manuela Pastoriza-Gallego,[†] Abdelghani Oukhaled,[†] Jean-Michel Betton,[‡] Loïc Auvray,[§] and Juan Pelta*[,†]

[†]LAMBE CNRS-UMR 8587, Université d'Evry and Université de Cergy-Pontoise, France

[‡]Unité de Biochimie Structurale, CNRS-URA Institut Pasteur, France

[§]Matière et Systèmes Complexes, CNRS-UMR 7057, Université Paris Diderot, France

Supporting Information

ABSTRACT: Understanding protein folding remains a challenge. A difficulty is to investigate experimentally all the conformations in the energy landscape. Only single molecule methods, fluorescence and force spectroscopy, allow observing individual molecules along their folding pathway. Here we observe that single-nanopore recording can be used as a new single molecule method to explore the unfolding transition and to examine the conformational space of native or variant proteins. We show that we can distinguish unfolded states from partially folded ones with the aerolysin pore. The unfolding transition curves of the destabilized variant are shifted toward the lower values of the denaturant agent compared to the wild type protein. The dynamics of the partially unfolded wild type protein follows a first-order transition. The denaturation curve obtained with the aerolysin pore is similar to that obtained with the α-hemolysin pore. The nanopore geometry or net charge does not influence the folding transition but changes the dynamics.

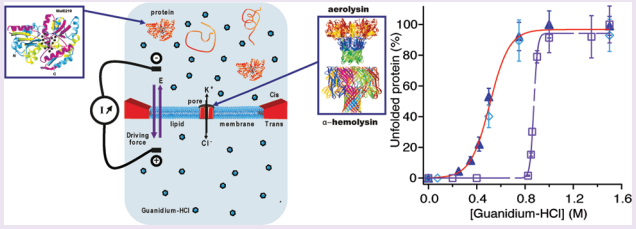

Understanding how proteins fold remains one of the fundamental problems in biology and physics.[1] This mechanism also has considerable medical relevance and potential applications. Many experimental methods, simulations, and theories explore protein folding mechanisms,[2,3] but one of the main difficulties is to access the conformational space experimentally. Two single-molecule methods have been used to study protein conformations, fluorescence spectroscopy[4] and AFM-bases force spectroscopy,[5] but neither permit the complete separation of all of the conformations. We propose another method to study the protein folding at the single molecule level using nanopores and electrical detection.

Biological or synthetic macromolecules can be electrically driven through a nanopore,[6−8] and this kind of manipulation is now widely used and has many important potential applications.[9−12] Nanopores have been used to study protein transport,[12−25] nanopore−protein interactions,[12,26−28] and protein−protein interactions[18,23] and recently to investigate protein conformations in different conditions.[20,21,28−31] Nevertheless, up to now, the conformational space of native or variant proteins and their unfolding transition using single-nanopore have been less studied.

We have previously shown, using the α-hemolysin pore and maltose binding protein (MBP or MalEwt), that unfolded proteins induce short current pore blockades and their frequency increases as the concentration of denaturing agent increases, following a sigmoidal denaturation curve. We have also observed very long blockades in channels associated with partially folded proteins.[21] Here, we study the destabilized variant of maltose binding protein unfolding through the vestibule and stem side entry of the α-hemolysin pore, and we compare the unfolding transition of the wild type and the destabilized variant. We study also the denaturation of MalEwt using a different channel, aerolysin, in order to probe the influence of the geometry or net charge of the channel in the folding transition.

The nanopore device used in our experiments is presented in Figure 1a. MalEwt or MBP is the maltose binding protein of *E. coli*. Its shape is ellipsoidal with overall dimensions of 3 × 4 × 6.5 nm^3.[32] The overall structure of MalE consists of two discontinuous domains constructed from secondary structural βαβ units and surrounding a cleft that forms the binding site for maltose and maltodextrins (Figure 1a). When the α/β loop connecting α-helix VII to β-strand J in the C-domain was modified (Gly220 and Glu221 simultaneously substituted by Asp and Pro), the resulting MalE219 variant is strongly destabilized and completely unfolded at low guanidium concentration.[33] The sizes and the net charges of MalEwt and the variant (MalE219) are the same: 370 residues (40707 Da) and −8*e*. The α-hemolysin channel is characterized by a geometric asymmetry due to the presence of a large extramembrane vestibule domain[34] and by a slightly positive global net charge (*Z* = +7e). The aerolysin pore is heptameric and

Received: November 17, 2011
Accepted: January 19, 2012
Published: January 19, 2012

   dx.doi.org/10.1021/cb2004737 | *ACS Chem. Biol.* 2012, 7, 652−658

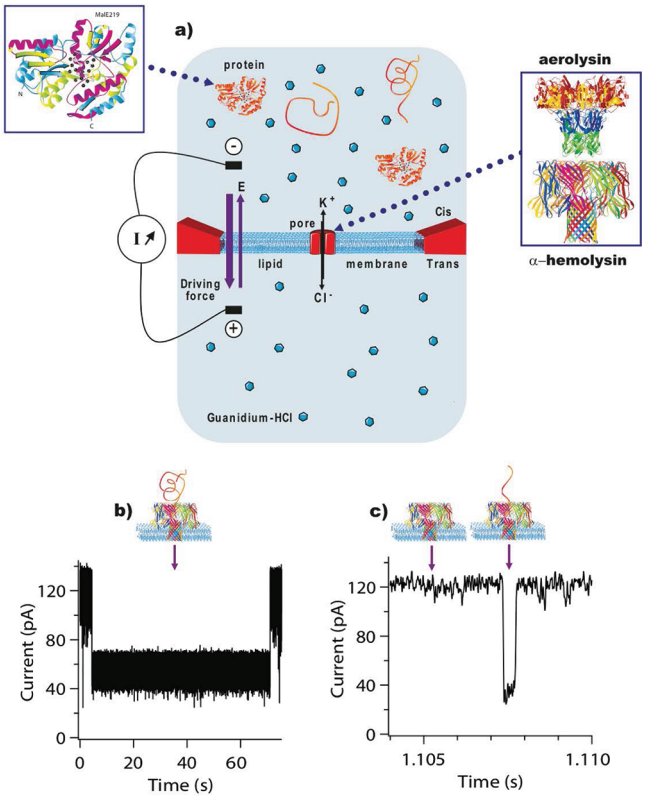

Figure 1. Principle of protein conformation detection using the nanopore device. Schematic representation of the nanopore device (a). One channel, α-hemolysin or aerolysin, is inserted in a suspended lipid bilayer. The lipid membrane is submitted to an electrical potential difference ,which induces a current in a single nanopore due to the presence of K^+ and Cl^- in the bulk solution and their diffusion through the nanopore. The proteins are added to one compartment of the chamber. The denaturing agent, guanidium chloride, is in both compartments at the same concentration. The data suggest that several different protein conformations are detected: partially folded and unfolded. Two proteins are used: the wild type maltose-binding protein (MalEwt) and a destabilized variant (MalE219). In our experimental conditions, the proteins are negatively charged. Detection of partially folded protein (b) or completely unfolded (c) MalE219, transport with the α-hemolysin nanopore. Part of a current trace obtained with V = 100 mV, [Gdm-HCl] = 0.35 M.

does not have a vestibule domain,[35] and its net charge is highly negative (Z = −52e). The length of both channels is the same, 10 nm, but the aerolysin pore diameter, estimated to be between 1 and 1.7 nm,[35] is smaller than the α-hemolysin one. In absence of protein, we do not observe any current blockade. We can measure the open pore conductance through the α-hemolysin pore, 120 ± 6 pA at 100 mV in the presence of 1 M KCl and 0.35 M Gdm-HCl (Figure 1c). When the destabilized MalE219 or the MalEwt proteins enter the channel, a decrease in current is observed, and the dwell time depends on the protein conformation. In the case of partially folded MalE219 protein at 0.35 M Gdm-HCl, the dwell time is very long; we observe $<t>$ = 75 ± 47 s (Figure 1b), and for an unfolded protein the mean blockade duration is short, $<t>$ = 208 ± 74 μs (Figure 1c). With the wild type protein we do not observe any current blockade at this Gdm-HCl concentration.

We have previously studied MalEwt unfolding through an α-hemolysin channel.[21] In order to probe the influence of channel structure, geometry, or net charge on protein unfolding detected by single-nanopore recording, we perform the MalEwt unfolding through a different pore, the aerolysin. Typical parts of current traces are presented in Figure 2a−c showing

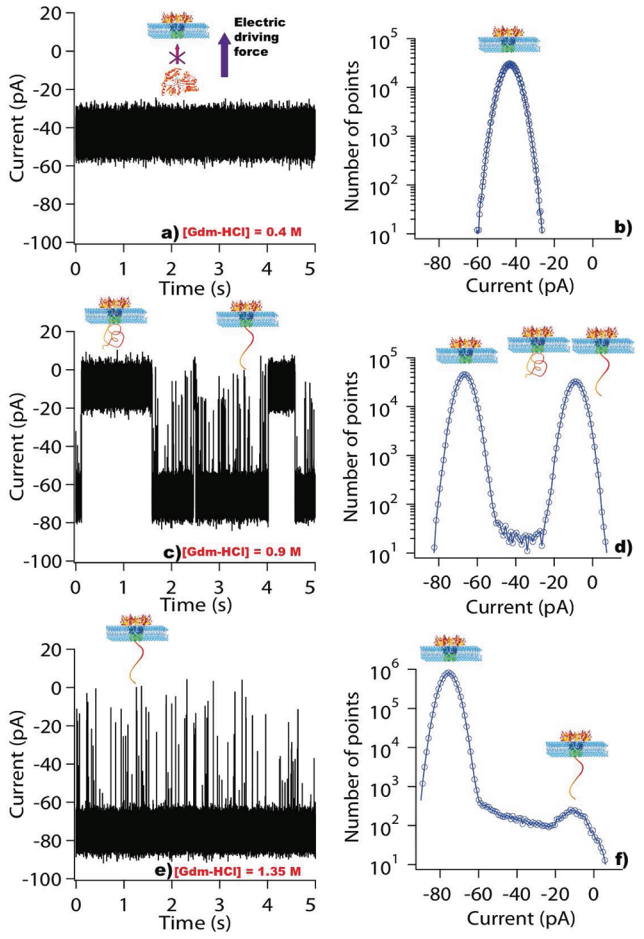

Figure 2. Electrical detection of protein unfolding through a single aerolysin nanopore as a function of guanidium chloride concentration. (a) At [Gdm-HCl] = 0.4 M, no current blockade is observed, and the folded native protein does not enter inside the nanopore. (c) At [Gdm-HCl] = 0.9 M, short current blockades coexist with long blockades for unfolded and partially folded proteins, respectively. (e) At [Gdm-HCl] = 1.35 M, only short current blockades are observed, and proteins are completely unfolded. (b, d, f) Current histograms of the number of points as a function of the current; the solid line is to guide the eye. At [Gdm-HCl] = 0.4 M, only one peak appears and corresponds to the open pore conductance (b). At [Gdm-HCl] = 0.9 M, a new peak is observed at low current corresponding to the protein chain inside the pore, and the current of the open pore conductance increases slightly (d). At [Gdm-HCl] = 1.35 M, two peaks are observed: one for an unfolded chain inside the channel and one due to the current of the empty pore (f). The applied voltage is V = −70 mV. Here the proteins are added in the trans compartment of the chamber.

electrical recording in the presence of proteins (MalEwt) for different denaturing agent concentrations between 0 and 1.5 M. After adding proteins, in the absence of Gdm-HCl (data not shown), or at low concentrations (Figure 2a), we do not observe any spikes during the time of the experiment (up to 2 h long). The wild type native protein does not enter the channel. At 0.9 M Gdm-HCl, long current blockades alternate with series of short ones (Figure 2b). In the presence of 1.35 M Gdm-HCl, the long blockades disappear, and the number of short duration events increases (Figure 2c). We assume that the

dx.doi.org/10.1021/cb2004737 | ACS Chem. Biol. 2012, 7, 652−658

long current blockades are associated with partially folded proteins and the short pore blockades with unfolded proteins. We observe an increase in the open pore conductance (Figure 2d–f) when the Gdm-HCl increases; this is due to a linear increase of solution conductivity from 0 to 1.5 M Gdm-HCl in 1 M KCl (data not shown). The mean blockade current is the same, $I_B = 9 \pm 3$ pA, for both types of event, the long blockades and the short ones (Figure 2e). This means that the unfolded part of the chain is inside the pore and the folded part of the protein is outside the pore. The long residence times are not due to a pore exit from the lipid bilayer or to a plugged channel. These times correspond to the duration required to mechanically unfold the partially folded proteins by the electrical field. For unfolded MalEwt proteins, we observe two types of event: bumping events, when a protein diffuses close to the pore, associated with a very short blockade time and low current pore blockade; and residence events with a long blockade time and high current pore blockade (see Supporting Information). For example we find, at 1.35 M Gdm-HCl (Figure 3b), $t_{straddling} = 66 \pm 31$ μs and $t_{residence} = 684 \pm 107$ μs. This residence time is independent of the Gdm-HCl concentration used, $\langle t_{residence[Gdm\text{-}HCl]} \rangle = 717 \pm 39$ μs (Figure 3c). Above the denaturant concentration at the folding transition, the duration of short current blockades is independent of the guanidium concentration, and these events correspond to unfolded proteins. We have recently shown that at 1.5 M Gdm-HCl concentration the residence time of unfolded MalEwt through an aerolysin channel is independent of protein concentration, $\langle t_{residence[protein]} \rangle = 732 \pm 31$ μs. Furthermore, this time decreases exponentially when the applied voltage increases, and duration increases with the chain length.[22] All of these results might strongly suggest that this residence time is a transport time. The variation of the event frequency of short blockades as a function of Gdm-HCl concentration has a sigmoidal dependency, reminiscent of an unfolding transition curve, between folded to unfolded state (Figure 3d). The denaturing agent concentration of the half denaturation is $C_{half} = 0.87 \pm 0.01$ M (Table 1). Unlike short blockades, the long current blockade duration decreases when the Gdm-HCl concentration increases to 1 M Gdm-HCl. The folded part of the chain, at the nanopore entry, is progressively unfolded by the denaturing agent. We show the coexistence of short and long current blockades for different Gdm-HCl concentrations, and the mean duration time scale is very large, between 700 ± 15 μs and 27 ± 24 s. In order to take into account the possible glassy dynamics in the protein folding processes,[21,36−38] we have plotted the long blockade duration according to a Vogel−Tamman−Fulcher law: $t_{long} = t_0 \exp[A/(C - C_g)]$ with C_g the denaturant concentration at the folding transition. A best fit yields $C_g = 0.81 \pm 0.01$ M, $\tau_0 = 38 \pm 25$ μs; $A = 0.56 \pm 0.12$ M (Figure 3f). This protein folding is associated with a first-order transition with a possible glassy behavior. Single-molecule force spectroscopy, when MalEwt is pulled at its termini, has shown the existence of three unfolding intermediates on the mechanical unfolding pathway. Four stable structural blocks were found.[39]

To compare the accuracy of the unfolding transition measure, we also studied the unfolding of MalE219, a destabilized variant of the maltose binding protein. We probed the unfolding process through the α-hemolysin channel; the proteins enter by the vestibule or stem side (Figure 4). We also compared its unfolding transition to that obtained with the wild type protein (MalEwt). When the protein enters the α-hemolysin pore either by the vestibule or by the stem side, the short current

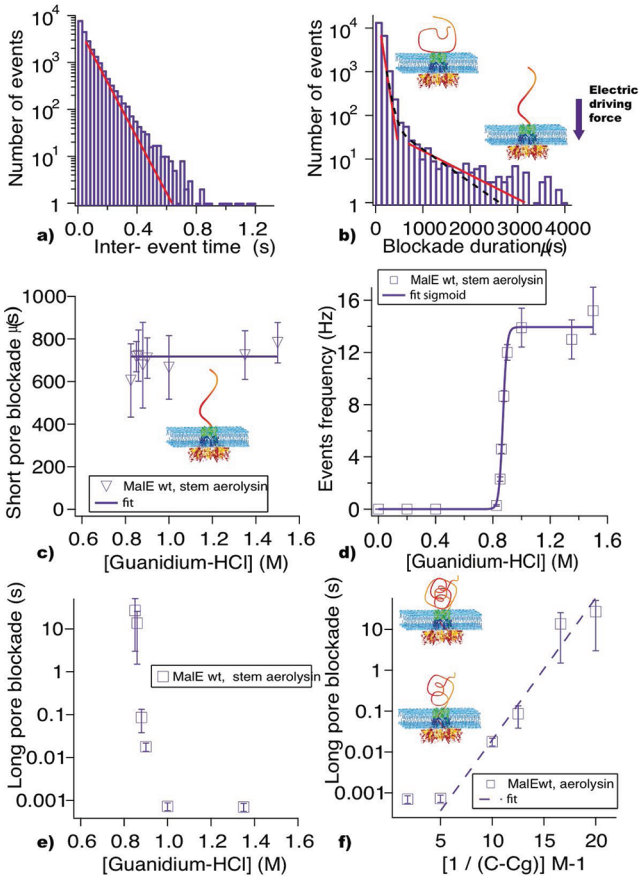

Figure 3. The aerolysin nanopore is a sensor to detect the unfolding of MalEwt. (a) Event frequency and (b) blockade duration determination for completely unfolded proteins at [Gdm-HCl] = 1.35 M. Distribution of interevent time (a), continuous line is exponential fit, semilog scale; distribution of blockade duration for MalEwt (b), continuous lines are single exponential fits, dotted lines correspond to a double exponential fit, semilog scale. (c) Short pore blockade duration of unfolded proteins as a function of guanidium chloride concentration; we found $\langle t_{short} \rangle = 717 \pm 39$ μs. Event frequency of short blockades as a function of guanidium chloride concentration. The line is a fit using a sigmoid function. No blockade is observed below [Gdm-HCl] = 0.8 M. (d) At the unfolding transition, event frequency increases sharply with [Gdm-HCl]. (e) Long pore blockade duration of partially unfolded proteins as a function of guanidium chloride concentration; their duration decreases sharply with the increase of [Gdm-HCl] up to 1 M. (f) Vogel−Tammann−Fulcher representation of long blockade duration versus $1/(C - C_g)$ with C = [Gdm-HCl] and $C_g = 0.8$ M. Dotted line is the best fit of the form $t = t_0 \exp(A/(C - C_g))$. The applied voltage is $V = -70$ mV.

Table 1. Fit Parameters of Events Frequency As a Function of Gdm-HCl Concentration (Figures 3d and 4b)[a]

	MalE 219 vestibule α-hemolysin	MalE 219 stem α-hemolysin	MalE wt stem aerolysin
C_{half} (M)	0.49 ± 0.01	0.52 ± 0.04	0.87 ± 0.01
F_{max} (Hz)	64 ± 2	33 ± 3.7	14 ± 1.1

[a] C_{half} (M) is the Gdn-HCl concentration at the midpoint of the unfolding transition of the protein, and F_{max} (Hz) is the events frequency maximal.

pore blockade durations are similar. The unfolded protein was more likely to enter the pore by the vestibule domain than by the stem side (Figure 4). For example, we obtain the following

dx.doi.org/10.1021/cb2004737 | ACS Chem. Biol. 2012, 7, 652−658

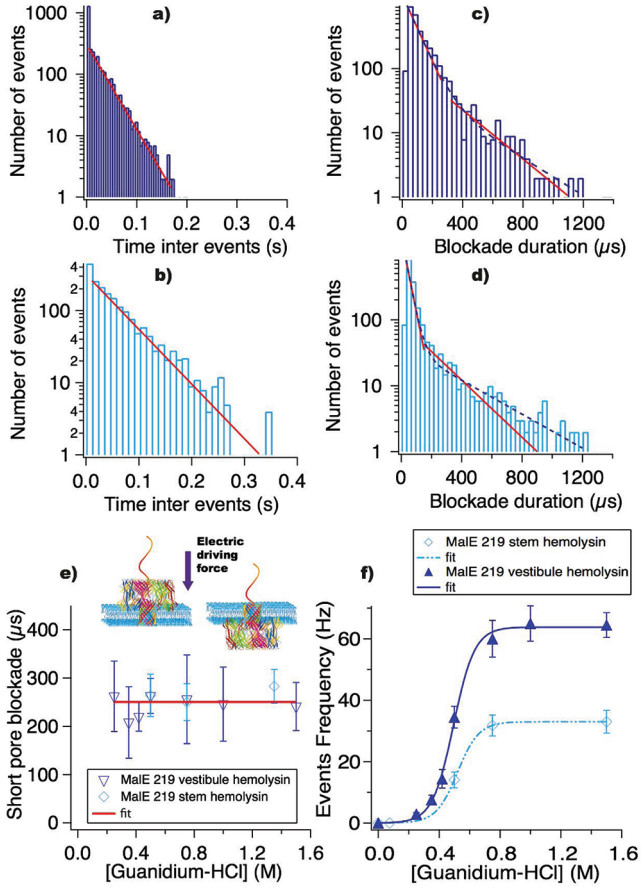

Figure 4. Variant protein unfolding through an α-hemolysin pore by the vestibule side or by the stem side entry. Examples of distribution of time between events (a, b) and blockade duration (c, d) obtained for one channel, when the molecules enter by the vestibule (a, c) or by the stem side of the channel (b, d), continuous lines are single exponential fits, dotted lines correspond to a double exponential fit, semilog scale, [Gdm-HCl] = 0.5 M. (e) Short pore blockade duration of unfolded MalE219 as a function of guanidium chloride concentration. The unfolded proteins enter the α-hemolysin channel either by the vestibule side or by the stem side; we found $<t_{short}>$ = 250 ± 14 μs. (f) Event frequency of short blockades as a function of guanidium chloride concentration. The line (continuous or dotted) is a fit using a sigmoid function. No blockade is observed below [Gdm-HCl] = 0.075 M. At the unfolding transition, event frequency increases with [Gdm-HCl].

at 0.5 M guanidium: $t_{unfolded\text{-}vestibule}$ = 265 μs ± 38 μs and $t_{unfolded\text{-}stem}$ = 282 μs ± 55 μs (Figure 4c,d) and $F_{vestibule}$ = 32 ± 1 Hz and F_{stem} = 17 ± 0.5 Hz (Figure 4a,b). We have previously shown that the average rate by which the unfolded protein MalEwt enters the pore depends on the side of addition,[40] as was shown for single-stranded DNA homopolymers and the α-hemolysin channel.[41]

The short current blockade time is also independent of the guanidium concentration; we find $<t_{residence}>$ 250 ± 14 μs (Figure 4e). With MalEwt, we had previously obtained $<t_{residence}>$ = 200 ± 100 μs[21] using the α-hemolysin pore. This residence time could be associated with a transport time of unfolded proteins. The dynamics of unfolded proteins are the same for MalE219 and MalEwt through the α-hemolysin channel, and this is also the case with the aerolysin pore.[22] The mean residence time of a protein is shorter with α-hemolysin than with the aerolysin channel. This is due to a different applied voltage and also to a different pore diameter. We apply V = 100 mV and V = −70 mV for the α-hemolysin and the aerolysin pore, respectively. When the proteins enter by the hemolysin vestibule side or by the stem side, the frequency of events follows a sigmoidal variation (Figure 4e). The denaturing agent concentration of the half transition for the destabilized variant is lower than that for the wild type protein (Table 1). The maximum event frequency is higher for MalE219 than for MalEwt (Table 1) due probably to a difference in the activation energy of unfolded proteins for entry into the channel. We have previously found that the activation energy of the α-hemolysin[21] is about half of that found for the aerolysin stem side entry.[22] In our experimental conditions, we observe long blockade durations only up to 0.42 M Gdm-HCl concentration for this destabilized variant protein.

Here we show that the nanopore approach associated to an electrical detection is a sensitive and powerful method to study protein folding. It allows to compare data obtained at several protein concentrations and applied voltages and using two different pores with different net charge, geometry, and structure. In order to compare all data, we have normalized the maximum event frequency to 100% of unfolded proteins. We obtain a single denaturation curve of MalE219 when the proteins enter by both sides of the α-hemolysin pore (Figure 5).

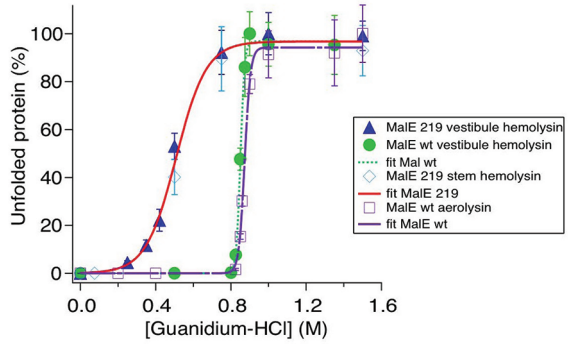

Figure 5. Unfolding curves at the single molecule level using different nanopores and different proteins. The events frequency is normalized to obtain this curve, and the percentages are calculated from these events. MalE219 is unfolded through the α-hemolysin pore when the molecules enter by the two sides of the channel, and MalEwt is unfolded through the aerolysin pore and with the α-hemolysin pore. The data are adapted from previous work.[21]

The Gdm-HCl concentration at the midpoint of the unfolding transition of this protein is C_{half} = 0.5 ± 0.01 (Table 2). The unfolding process through a nanopore does not depend on the channel entry side. The denaturation curve of MalEwt obtained with the aerolysin channel is similar within the standard

Table 2. Fit Parameters of Unfolded Protein as a Function of Gdm-HCl Concentration (Figure 4c)[a]

	MalE 219 α-hemolysin	MalE wt aerolysin	MalE wt α-hemolysin
C_{half} (M)	0.5 ± 0.01	0.87 ± 0.01	0.85 ± 0.01
unfolded protein maximal (%)	97 ± 3.5	94 ± 4.5	97 ± 5.6

[a] C_{half} (M) is the Gdn-HCl concentration at the midpoint of the unfolding transition of the protein.

dx.doi.org/10.1021/cb2004737 | ACS Chem. Biol. 2012, 7, 652–658

deviation to that found previously with an α-hemolysin pore[21] (Figure 5, Table 2). We obtain, with the aerolysin or α-hemolysin channel, at the midpoint of the unfolding transition of MalEwt: $C_{half\text{-}aerolysin}$ = 0.87 ± 0.01 M and $C_{half\text{-}hemolysin}$ = 0.85 ± 0.01 M. We show that the protein unfolding process is independent of the geometry, net charge, and structure of the nanopore.

In bulk experiments, the Gdm-HCl concentrations at the midpoint of the unfolding transition of MalE219 and MalEwt are, respectively, C_{half} = 0.35 ± 0.01 M and C_{half} = 1.05 ± 0.05 M.[33] The difference obtained by single-nanopore recording and bulk experiments could be due to the tryptophan fluorescence emission of different protein conformations that could not be separated in the bulk. Another explanation for this difference is that at medium Gdm-HCl concentrations, the applied electrical force could be enough to unfold a small part of secondary structure inside the protein.

In the future we will perform NMR experiments as a function of Gdm-HCl concentrations in order to investigate the structure of the protein along the folding pathway in relation with the current blockades in channels.

In conclusion, we compared the unfolding transition of the wild type and a destabilized variant of maltose binding protein using two different channels, α-hemolysin and aerolysin. For the two channels, unfolded proteins induce short blockades, and their frequency increases as the concentration of denaturing agent increases, following a sigmoidal unfolding curve. Their duration is constant as a function of the concentration of denaturing agent. Partially folded proteins exhibit very long blockades in nanopores. The blockade duration decrease when the concentration of denaturing agent increases. For the wild type protein, the variation of the long blockade duration as a function of denaturant concentration is well described by a Vogel−Tamman−Fulcher relationship, and this dependency could be associated to a possible glassy behavior. The MalEwt unfolding curve obtained using the aerolysin channel is similar to that previously obtained with the α-hemolysin pore. We find that the unfolding denaturation curves of the destabilized variant are the same through the vestibule and stem side entry of the α-hemolysin pore and are shifted toward the lower values of the denaturant agent compared to the wild type protein. We prove that the nanopore structure, geometry, and the net charge do not influence the folding transition but change the dynamics. We show a new method at single-molecule level to study protein folding and protein stability. This method is highly sensitive to obtain an unfolding curve, to detect protein mutations, to investigate protein stability as a function of environment, and to observe different protein conformations along the folding pathway. The nanopore device also provides prospects concerning the protein unfolding by other denaturing agents or the interaction between proteins. The control of protein unfolding through a nanopore is also a crucial step for a potential application concerning ultrafast sequencing of proteins.

METHODS

Membrane lipid bilayers were made by using the previously described method.[42] In brief, a film of a 1% solution of diphytanoylphosphatidylcholine-lecithin (Avanti) in decane is spread across a 150 μm wide hole drilled in a polysulfone wall separating the two compartments of a chamber. Each compartment contains 1 mL of 1 M KCl, 5 mM HEPES, pH 7.5. After thinning of the decane film and formation of a planar bilayer, one channel is inserted by adding monomeric α-hemolysin (Sigma) or recombinant aerolysin from a stock solution in one compartment. Aerolysin was produced in *E. coli* as proaerolysin as described before[43] and was activated by digestion with trypsin for 10 min at RT to eliminate the propeptide sequence, allowing monomers to polymerize.[44]

The production and purification of the recombinant maltose binding protein of *E. coli* (MalE) and the strongly destabilized variant MalE219 have been described previously.[45] In the experiments, the final protein concentrations are 0.35 μM with the α-hemolysin channel or 3 μM with the aerolysin channel.

The ionic current through a single α-hemolysin or aerolysin channel was measured using an Axopatch 200B amplifier. Data were filtered at 10 kHz (100 μs) and acquired at 250 kHz intervals (4 μs) using the DigiData 1322A digitizer with Clampex software (Axon Instruments, Union City, CA, USA). The measurements of the transients were based on the statistical analysis of the current traces. Data were systematically checked for reproducibility with several pores. The main difficulty of data analysis is to separate the pulses of electric current from the noise. We define a first threshold th1 as the mean current of the open pore $<I_0>$ minus twice the standard deviation σ of its distribution, th1 = $<I_0> - 2\sigma$. We define a second threshold th2 as the end of this distribution. The average frequency of blockades is deduced from the distribution of the time intervals T_i between two successive blockades. The average duration of blockades is deduced from the distribution of blockade duration T_t. The two blockade time distributions of independent events are adjusted with 2 separate exponential functions, $y = A_1 \exp(-t/\tau_1)$ and $y = A_2 \exp(-t/\tau_2)$ and with a double exponential function, $y = A_1 \exp(-t/\tau_1) + A_2 \exp(-t/\tau_2)$. Each blockade duration is the average of the two characteristic times. All statistical analyses were performed using Igor Pro software (WaveMetrics Inc.).

ASSOCIATED CONTENT

Supporting Information

This material is available free of charge *via* the Internet at http://pubs.acs.org.

AUTHOR INFORMATION

Corresponding Author

*E-mail: jpelta@univ-evry.fr.

Author Contributions

#These authors contributed equally to this work.

Notes

The authors declare no competing financial interest.

ACKNOWLEDGMENTS

This work was supported by grant funding from the Action Thématique Incitative Genopole, PCV prise de risques CNRS and ANR Blanche "TRANSFOLDPROT" BLAN08-1_339991. We thank Gisou Van der Goot (Ecole Polytechnique Lausanne) for the gift of the vector for recombinant aerolysin production and Marie Wagmann for the figure design graphics. We thank Kari Foster for kindly correcting the language of the manuscript.

REFERENCES

(1) Dobson, C. M. (2003) Protein folding and misfolding. *Nature 426*, 884−890.

(2) Bartlett, A. I., and Radford, S. E. (2009) An expanding arsenal of experimental methods yields an explosion of insights into protein folding mechanisms. *Nat. Struct. Mol. Biol. 16*, 582−588.

(3) Freddolino, P. L., Harrison, C. B., Liu, Y., and Schulten, K. (2010) Challenges in protein-folding simulations. *Nat. Phys. 6*, 751−758.

(4) Michalet, X., Weiss, S., and Jager, M. (2006) Single-molecule fluorescence studies of protein folding and conformational dynamics. *Chem. Rev. 106*, 1785−1813.

(5) Fisher, T. E., Marszalek, P. E., and Fernandez, J. M. (2000) Stretching single molecules into novel conformations using the atomic force microscope. *Nat. Struct. Biol. 7*, 719−724.
(6) Kasianowicz, J. J., Brandin, E., Branton, D., and Deamer, D. W. (1996) Characterization of individual polynucleotide molecules using a membrane channel. *Proc. Natl. Acad. Sci. U.S.A. 93*, 13770−13773.
(7) Reiner, J. E., Kasianowicz, J. J., Nablo, B. J., and Robertson, J. W. F. (2010) Theory for polymer analysis using nanopore-based single-molecule mass spectrometry. *Proc. Natl. Acad. Sci. U.S.A. 107*, 12080−12085.
(8) Robertson, J. W. F., Rodrigues, C. G., Stanford, V. M., Rubinson, K. A., Krasilnikov, O. V., and Kasianowicz, J. J. (2007) Single-molecule mass spectrometry in solution using a solitary nanopore. *Proc. Natl. Acad. Sci. U.S.A. 104*, 8207−8211.
(9) Branton, D., Deamer, D. W., Marziali, A., Bayley, H., Benner, S. A., Butler, T., Di Ventra, M., Garaj, S., Hibbs, A., Huang, X., Jovanovich, S. B., Krstic, P. S., Lindsay, S., Ling, X. S., Mastrangelo, C. H., Meller, A., Oliver, J. S., Pershin, Y. V., Ramsey, J. M., Riehn, R., Soni, G. V., Tabard-Cossa, V., Wanunu, M., Wiggin, M., and Schloss, J. A. (2008) The potential and challenges of nanopore sequencing. *Nat. Biotechnol. 26*, 1146−1153.
(10) Howorka, S., and Siwy, Z. S. (2009) Nanopore analytics: sensing of single molecules. *Chem. Soc. Rev. 38*, 2360−2384.
(11) Kasianowicz, J. J., Robertson, J. W. F., Chan, E. R., Reiner, J. E., and Stanford, V. M. (2008) Nanoscopic porous sensors. *Ann. Rev. Anal. Chem. 1*, 737.
(12) Movileanu, L. (2009) Interrogating single proteins through nanopores: challenges and opportunities. *Trends Biotechnol. 27*, 333−341.
(13) Han, A., Schurmann, G., Mondin, G., Bitterli, R. A., Hegelbach, N. G., de Rooij, N. F., and Staufer, U. (2006) Sensing protein molecules using nanofabricated pores. *Appl. Phys. Lett. 88*, 093901−093903.
(14) Sutherland, T. C., Long, Y. T., Stefureac, R. I., Bediako-Amoa, I., Kraatz, H. B., and Lee, J. S. (2004) Structure of peptides investigated by nanopore analysis. *Nano Lett. 4*, 1273−1277.
(15) Ammenti, A., Cecconi, F., Marini Bettolo, M. U., and Vulpiani, A. (2009) A statistical model for translocation of structured polypeptide chains through nanopores. *J. Phys. Chem. B 113*, 10348−10356.
(16) Firnkes, M., Pedone, D., Knezevic, J., Doblinger, M., and Rant, U. (2010) Electrically facilitated translocations of proteins through silicon nitride nanopores: conjoint and competitive action of diffusion, electrophoresis, and electroosmosis. *Nano Lett. 10*, 2162−2167.
(17) Fologea, D., Ledden, B., McNabb, D. S., and Li, J. (2007) Electrical characterization of protein molecules by a solid-state nanopore. *Appl. Phys. Lett. 91*, nihpa38991.
(18) Han, A., Creus, M., Schürmann, G., Linder, V., Ward, T. R., de Rooij, N. F., and Staufer, U. (2008) Label-free detection of single protein molecules and protein−protein interactions using synthetic nanopores. *Anal. Chem. 80*, 4651−4658.
(19) Makarov, D. E. (2008) Computer simulations and theory of protein translocation. *Acc. Chem. Res. 42*, 281−289.
(20) Oukhaled, A., Cressiot, B., Bacri, L., Pastoriza-Gallego, M., Betton, J. M., Bourhis, E., Jede, R., Gierak, J., Auvray, L., and Pelta, J. (2011) Dynamics of completely unfolded and native proteins through solid-state nanopores as a function of electric driving force. *ACS Nano 5*, 3628−3638.
(21) Oukhaled, G., Mathe, J., Biance, A. L., Bacri, L., Betton, J. M., Lairez, D., Pelta, J., and Auvray, L. (2007) Unfolding of proteins and long transient conformations detected by single nanopore recording. *Phys. Rev. Lett. 98*, 158101−158104.
(22) Pastoriza-Gallego, M., Rabah, L., Gibrat, G., Thiebot, B., van der Goot, F. G., Auvray, L., Betton, J. M., and Pelta, J. (2011) Dynamics of unfolded protein transport through an aerolysin pore. *J. Am. Chem. Soc. 133*, 2923−2931.
(23) Sexton, L. T., Horne, L. P., Sherrill, S. A., Bishop, G. W., Baker, L. A., and Martin, C. R. (2007) Resistive-pulse studies of proteins and protein/antibody complexes using a conical nanotube sensor. *J. Am. Chem. Soc. 129*, 13144−13152.
(24) Yusko, E. C., Johnson, J. M., Majd, S., Prangkio, P., Rollings, R. C., Li, J., Yang, J., and Mayer, M. (2011) Controlling protein translocation through nanopores with bio-inspired fluid walls. *Nat. Nanotechnol. 6*, 253−260.
(25) Kowalczyk, S. W., Kapinos, L., Blosser, T. R., Magalhaes, T., van Nies, P., Lim, R. Y., and Dekker, C. (2011) Single-molecule transport across an individual biomimetic nuclear pore complex. *Nat. Nanotechnol. 6*, 433−438.
(26) Niedzwiecki, D. J., Grazul, J., and Movileanu, L. (2010) Single-molecule observation of protein adsorption onto an inorganic surface. *J. Am. Chem. Soc. 132*, 10816−10822.
(27) Sexton, L. T., Mukaibo, H., Katira, P., Hess, H., Sherrill, S. A., Horne, L. P., and Martin, C. R. (2010) An adsorption-based model for pulse duration in resistive-pulse protein sensing. *J. Am. Chem. Soc. 132*, 6755−6763.
(28) Christensen, C., Baran, C., Krasniqi, B., Stefureac, R. I., Nokhrin, S., and Lee, J. S. (2011) Effect of charge, topology and orientation of the electric field on the interaction of peptides with the α-hemolysin pore. *J. Peptide Sci. 17*, 726−734.
(29) Freedman, K. J., Jurgens, M., Prabhu, A., Ahn, C. W., Jemth, P., Edel, J. B., and Kim, M. J. (2011) Chemical, thermal, and electric field induced unfolding of single protein molecules studied using nanopores. *Anal. Chem. 83*, 5137−5144.
(30) Stefureac, R., Waldner, L., Howard, P., and Lee, J. S. (2008) Nanopore analysis of a small 86-residue protein. *Small 4*, 59−63.
(31) Talaga, D. S., and Li, J. (2009) Single-molecule protein unfolding in solid state nanopores. *J. Am. Chem. Soc. 131*, 9287−9297.
(32) Spurlino, J. C., Lu, G. Y., and Quiocho, F. A. (1991) The 2.3-A resolution structure of the maltose- or maltodextrin-binding protein, a primary receptor of bacterial active transport and chemotaxis. *J. Biol. Chem. 266*, 5202−5219.
(33) Raffy, S., Sassoon, N., Hofnung, M., and Betton, J. M. (1998) Tertiary structure-dependence of misfolding substitutions in loops of the maltose-binding protein. *Protein Sci. 7*, 2136−2142.
(34) Song, L., Hobaugh, M. R., Shustak, C., Cheley, S., Bayley, H., and Gouaux, J. E. (1996) Structure of staphylococcal alpha-hemolysin, a heptameric transmembrane pore. *Science 274*, 1859−1866.
(35) Parker, M. W., Buckley, J. T., Postma, J. P., Tucker, A. D., Leonard, K., Pattus, F., and Tsernoglou, D. (1994) Structure of the Aeromonas toxin proaerolysin in its water-soluble and membrane-channel states. *Nature 367*, 292−295.
(36) Brujic, J., Hermans, Z., Walther, K. A., and Fernandez, J. M. (2006) Single-molecule force spectroscopy reveals signatures of glassy dynamics in the energy landscape of ubiquitin. *Nat. Phys.*, 282−286.
(37) Frauenfelder, H., Sligar, S. G., and Wolynes, P. G. (1991) The energy landscapes and motions of proteins. *Science 254*, 1598−1603.
(38) Iben, I. E., Braunstein, D., Doster, W., Frauenfelder, H., Hong, M. K., Johnson, J. B., Luck, S., Ormos, P., Schulte, A., Steinbach, P. J., Xie, A. H., and Young, R. D. (1989) Glassy behavior of a protein. *Phys. Rev. Lett. 62*, 1916−1919.
(39) Bertz, M., and Rief, M. (2008) Mechanical unfoldons as building blocks of maltose-binding protein. *J. Mol. Biol. 378*, 447−458.
(40) Pastoriza-Gallego, M., Gibrat, G., Thiebot, B., Betton, J. M., and Pelta, J. (2009) Polyelectrolyte and unfolded protein pore entrance depends on the pore geometry. *Biochim. Biophys. Acta 1788*, 1377−1386.
(41) Henrickson, S. E., Misakian, M., Robertson, B., and Kasianowicz, J. J. (2000) Driven DNA transport into an asymmetric nanometer-scale pore. *Phys. Rev. Lett. 85*, 3057−3060.
(42) Montal, M., and Mueller, P. (1972) Formation of bimolecular membranes from lipid monolayers and a study of their electrical properties. *Proc. Natl. Acad. Sci. U.S.A. 69*, 3561−3566.
(43) Moniatte, M., van der Goot, F. G., Buckley, J. T., Pattus, F., and van Dorsselaer, A. (1996) Characterisation of the heptameric pore-forming complex of the Aeromonas toxin aerolysin using MALDI-TOF mass spectrometry. *FEBS Lett. 384*, 269−272.

(44) Cabiaux, V., Buckley, J. T., Wattiez, R., Ruysschaert, J. M., Parker, M. W., and van der Goot, F. G. (1997) Conformational changes in aerolysin during the transition from the water-soluble protoxin to the membrane channel. *Biochemistry 36*, 15224−15232.
(45) Betton, J. M., and Hofnung, M. (1996) Folding of a mutant maltose-binding protein of Escherichia coli which forms inclusion bodies. *J. Biol. Chem. 271*, 8046−8052.